Visual Abstract

Failure analysis of boron steel components for automotive applications

Marco V. Boniardi, Andrea Casaroli, Laura Sirangelo
Dipartimento di Meccanica, Politecnico di Milano, via La Masa 1, 20156 Milano, Italy
marco.boniardi@polimi.it, andrea.casaroli@polimi.it, laura.sirangelo@mail.polimi.it

Sergio Monella, Michele Mazzola
Bodycote Trattamenti Termici S.p.A., via Carso 89, 25050 Madone (Bg), Italy
sergio.monella@bodycote.com, michele.mazzola@bodycote.com

ABSTRACT. The automotive industry is continuously looking for an innovative mix of new steels and manufacturing techniques in order to improve process chain efficiency and cost reduction. To this aim, boron steels are becoming increasingly popular thanks to their high hardenability and machinability. Due to their reduced finishing steps, boron steels are commonly processed using fine blanking technologies.
The success of fine blanking on boron steel components is due to heat treatments which must be carefully designed to avoid precipitation of boron-rich compounds that would lower steel hardenability. At high temperature, boron is very reactive with oxygen and nitrogen.
The main focus of this paper is to show some drawbacks that can occur during heat treatments of automotive components. An experimental campaign was performed on two different boron steels, namely EN 34MnB5 and EN 22MnB5. The steel samples were previously spheroidized annealed in a neutral environment (hydrogen/nitrogen atmosphere), and then fine blanked to obtain specific automotive components which were subsequently quenched and tempered. Experimental tests revealed precipitation of nanometric compounds, causing strong grain refinement and localized decrease of steel hardenability. Hardenability problems were brought back to nitrogen pick-up during initial spheroidize annealing treatments.

KEYWORDS. Boron steel, Fine blanking, Spheroidize annealing, Nitrogen pick-up, Hardenability problems.

OPEN ACCESS

Citation: Boniardi, M. V., Casaroli, A., Sirangelo L., Monella S., Mazzola M., Failure analysis of Boron Steel Components for Automotive Applications, Frattura ed Integrità Strutturale, 64 (2023) 137-147.

Received: 11.01.2023
Accepted: 03.02.2023
Online first: 06.02.2023
Published: 01.04.2023

Introduction

Nowadays the automotive industry is facing the great challenge of further efficientizing its processes with improved performances. The main goals are to create lightweight components featuring the same levels of toughness and strength, and to reduce production steps. To reach these objectives, both new manufacturing techniques and new materials have to be developed. As to materials, low alloy steels are the most used in this sector due to their favorable combination of strength and ductility after quenching and tempering. A correct response to heat treatments being very important for these steels, boron steels have become very popular in the last decades. The addition of even small quantities of boron dramatically increases hardenability [1]. The so-called "Boron Effect" not only relies on the non-equilibrium segregation of boron atoms at ferrite grain boundaries to decrease energy and iron self-diffusion in these areas [2, 3], but also reduces the favorable nucleation sites for ferrite by hindering their formation and promoting the creation of martensite. In terms of hardenability, the addition of 0.001-0.003ppm (in weight) of boron to steel is equivalent to adding 0.6% Mn or 0.7% Cr or 0.5% Mo or 1.5% Ni (in weight) [4]. Boron steels provide an effective solution to increase hardenability but, at the same time, the alloy has to be carefully designed. Boron is very reactive with oxygen and nitrogen; consequently it is important to avoid the formation of oxides and precipitates that would prevent boron from increasing steel hardenability [5]. For what concerns manufacturing, blanking is a widely used technique even though almost all manufacturers find it difficult to cut high strength steel sheets. For this reason, a new technique, called fine blanking, is rapidly gaining ground [6]. Fine blanking is well known as an effective and economical shearing process that achieves both high precision and surface quality. It also cuts out the need for secondary operations, thereby lowering energy consumption and time waste. Fine blanking maximizes service strength and minimizes peak contact pressure to extend tool life [7]. Usually, hot or cold rolled strips and sheets have to be spheroidized annealed to decrease hardness [8]. After fine blanking, components are quenched and tempered to reach the desired hardness, yield strength and ultimate tensile strength. In these applications, spheroidize annealing must always take place in a protective atmosphere to avoid surface oxidation. One of the commonest techniques used today is the H_2-N_2 protective atmosphere [9] obtained from the dissociation of ammonia (NH_3). This solution is quite inexpensive, but nitrogen atoms may be present and absorbed by the components. This work intends to analyse the issues resulting from the combination of the commonest heat treatments performed on boron steels before and after fine blanking, with the other steps of the production chain.

Experimental setup

The components under investigation are part of the seat mechanisms. They are of the utmost importance for the safety of both the driver and the passengers because they absorb the kinetic energy produced during the crash. Their shapes being hard to obtain without many secondary treatments, the use of fine blanking is rapidly spreading in the manufacture of these types of items. The parts investigated have different geometries, similar to those shown in Fig. 1, and are made of two different boron steels, namely EN 34MnB5 and EN 22MnB5.

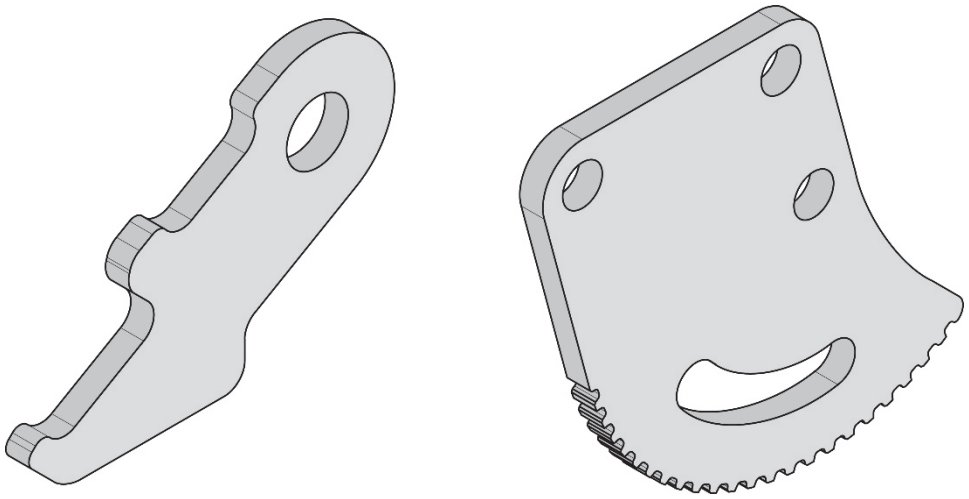

Figure 1: Examples of components used in the seat mechanisms.

The components under investigation come from the production cycle specified in Fig. 2. A 6.5mm thick steel sheet is pickled and spheroidized annealed a first time at 700°C in a Hydrogen-Nitrogen protective atmosphere. After the first annealing, the steel sheet is cold rolled to a thickness of 4.5mm, skin passed and spheroidized annealed a second time (H_2-N_2 protective atmosphere, at 700°C). Then, the components are cut from the steel sheet by means of fine blanking, quenched and tempered (Q&T) at a quenching temperature of 880°C, cooled in a salt bath, and tempered at 200°C.

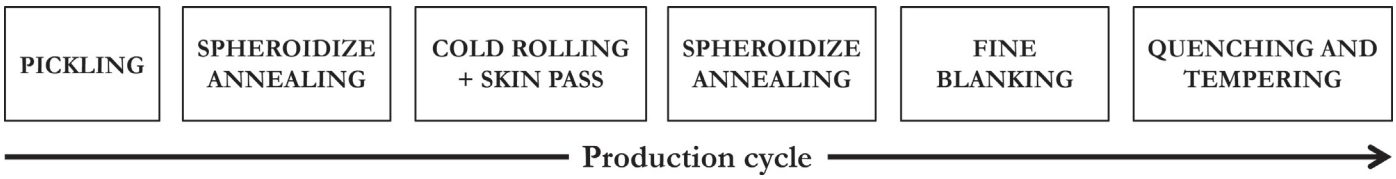

Figure 2: Production cycle of the components under investigation.

After Q&T, some components showed non-conformity due to decreased hardness (approx. 150HV down to a depth of 0.7mm) at the top layer of both sides of the components. The following paragraphs describe the tests performed and the equipment used for the failure analysis.

Experimental Equipment

Three types of tests were performed to understand the root-cause of the non-conformity:

1. *Microstructure Analysis*. Samples were polished, chemically etched using Nital2 and observed with both an optical microscope (Leica® DM4000) and a scanning electron microscope (Gemini Sigma 500). Analyses were performed to reveal the microstructure, grain size, type and morphology of the precipitates and any decarburization phenomena.
2. *Hardness Evaluation*. Hardness was evaluated using an FM-700 type micro Vickers hardness tester. Tests were performed all along the thickness of the samples to appreciate the hardness values after different types of heat treatments and manufacturing processes.
3. *Chemical Analysis*. The chemical composition was analysed by optical emission spectrometry (OES) using a SPECTROLAB stationary analyser. Tests were performed at increasing distances from the surface to evaluate the amount of carbon and boron all along the thickness of the samples subjected to different types of heat treatments.

Sample Selection

Tests were conducted on three different sets of samples, as listed below.

Set #1 consisted of Q&T samples, made of EN 34MnB5 steel and exhibiting the non-conformity. The goal of these tests was to better understand the nature of surface hardness impairment. Analyses were performed along three different edges, namely the two rolled edges (edge 1 and edge 2) and the cutting edge (edge 3). Two different configurations were used: in sample 1.1, edge 1 was ground to a depth of 0.7mm from the surface (Fig. 3), while in samples 0.X no grinding was involved.

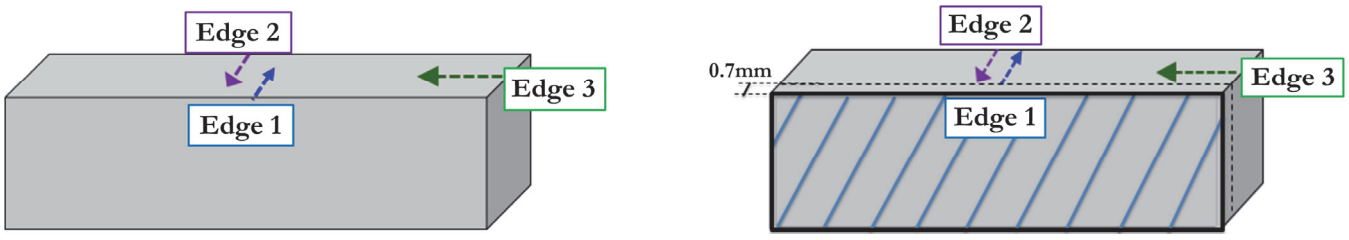

Figure 3: Analysed areas in samples from Set #1. Edges 1 and 2 correspond to the rolled surface; edge 3 corresponds to the area where the original rolled surface has been removed by fine blanking. In sample 1.1, edge 1 was ground to a depth of 0.7mm from the surface, while in samples 0.X no grinding was involved.

Set #1 included 5 samples, of which 4 in configuration 0.X and 1 in configuration 1.1. Tab. 1 shows the heat treatments applied to each sample.

Set #2 consisted of two series of three samples made of EN 34MnB5 steel and sectioned at different stages of the production cycle. In this second case, our main goal was to understand in which production phase the non-conformity originated. Samples were analysed "as untreated", i.e. subjected to the standard work sequence to the time of sampling (A.X series), and "as treated", i.e. after quenching at 880°C and tempering at 200°C in addition to the standard work sequence (A.X.1 series). Tab. 2 shows the work sequence adopted for each sample.

Sample	Heat Treatments
0.1	Quenching at 880°C and Tempering at 200°C
0.2	Sample 0.1 subjected to second Quenching at 880°C and Tempering at 200°C
0.3	Quenching at 880°C and Tempering at 200°C
0.4	Sample 0.3 subjected to Spheroidize annealing at 700°C, Quenching at 880°C and Tempering at 200°C
1.1	Quenching at 880°C and Tempering at 200°C

Table 1: Heat treatments applied to samples in Set #1.

Sample	Work Sequence
A.1	As Rolled + Pickling
A.2	As Rolled + Pickling + Spheroidize annealing at 700°C
A.3	As Rolled + Pickling + Spheroidize annealing at 700°C + Cold Rolling + Spheroidize annealing at 700°C
A.1.1	As Rolled + Pickling + Quenching at 880°C and Tempering at 200°C
A.2.1	As Rolled + Pickling + Spheroidize annealing at 700°C + Quenching at 880°C and Tempering at 200°C
A.3.1	As Rolled + Pickling + Spheroidize annealing at 700°C + Cold Rolling + Spheroidize annealing at 700°C + + Quenching at 880°C and Tempering at 200°C

Table 2: Work sequence adopted for samples in Set #2.

Set #3 consisted of two series, each including five samples made of EN 22MnB5 steel. The samples went through the production process before fine blanking (As Rolled + Pickling + First Spheroidize annealing at 700°C + Cold Rolling + Second Spheroidize annealing at 700°C) at two different times. The first batch (B.1) was used to manufacture non-compliant components, while the second batch (B.2) was used to manufacture components compliant with the minimum surface hardness requirement after Q&T. The two series of steel samples were quenched and tempered in the same furnace at the same time. The purpose of these tests was to clarify the effect of the production cycle on non-conformities before Q&T.

RESULTS AND DISCUSSION

Set #1

Fig. 4 shows the hardness values for the samples in Set #1. All 0.X samples exhibit a strong decrease in surface hardness (100-150HV) at the rolled surface (edge 1 and edge 2) to a depth of 0.5-0.7mm. On the other hand, only a minor hardness decrease is observed along the cutting edge (edge 3), where the original rolled surface was removed by fine blanking [10] before Q&T. The type of heat treatment has only limitedly affected the decrease in surface hardness. All 0.X samples are non-compliant even if the component has been Q&T twice (Fig. 4b) or if the Q&T process was preceded by spheroidize annealing at 700°C (Fig. 4d). Sample 1.1, instead, exhibits a different behavior. In this case, only edge 2 shows a hardness decrease, while edge 1, ground to a depth of 0.7mm from the surface before Q&T, is compliant all along its thickness (Fig. 4f). Furthermore, the loss of hardness at edge 2 is lower than in the previous case (< 100HV), which is due to lower thickness of the sample that (as already mentioned) was ground before Q&T. In these conditions, the quenching cooling phase is faster and heat treatment severity is more intense. Fig. 5 shows the micrographs of 0.X samples. The images highlight a layer of extremely fine ferrite and pearlite in the areas below the surface affected by the loss of hardness. On the other hand, areas far from the surface show only martensite. As expected, the layer of ferrite and pearlite is clearly visible under edges 1 and 2 while its thickness is low under edge 3.
The metallographic analyses confirm what was observed from the micro-hardness of sample 1.1, i.e. ferrite and pearlite disappear completely along edge 1 while they are still present at edge 2.

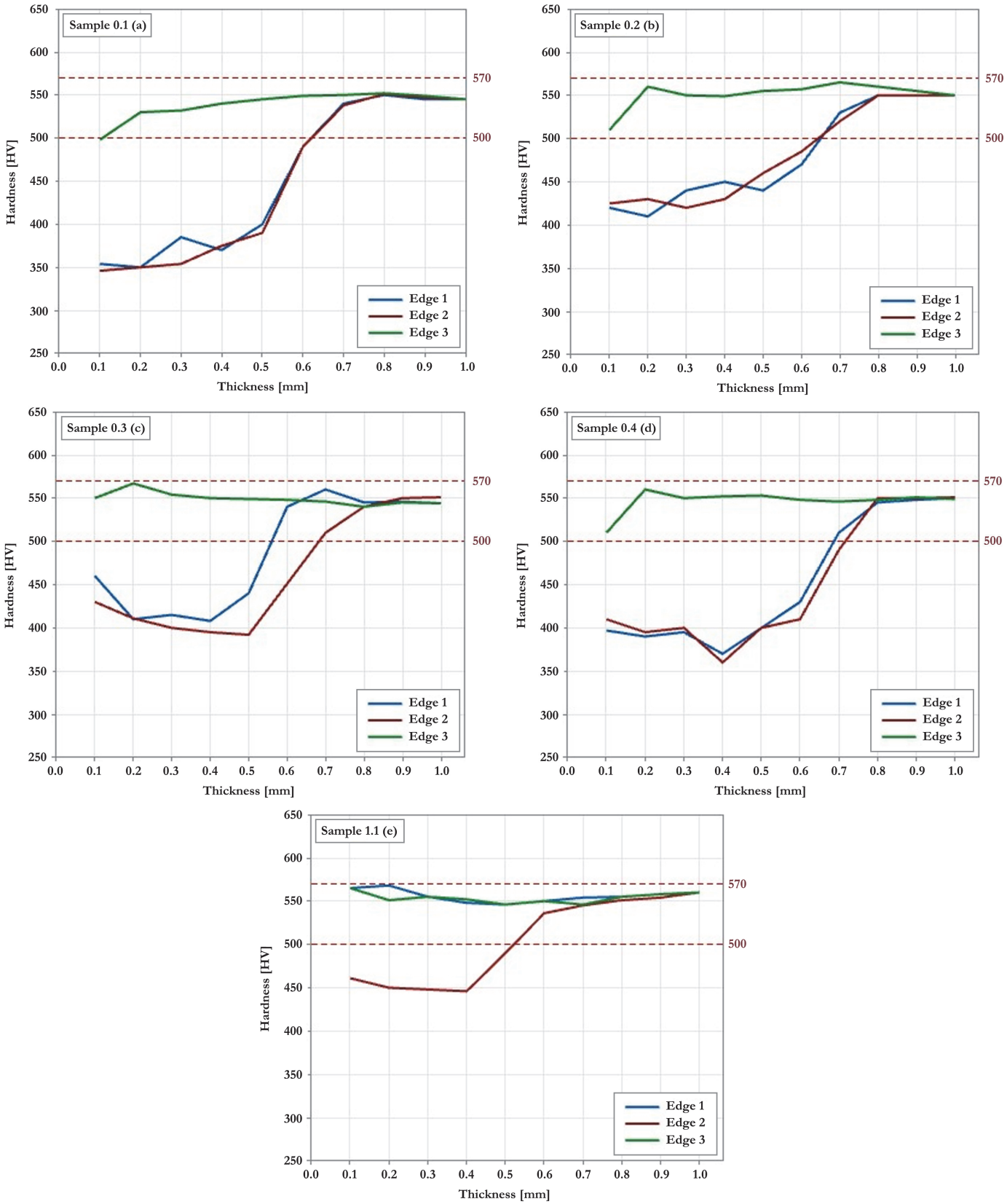

Figure 4: Hardness vs thickness in samples from Set #1.

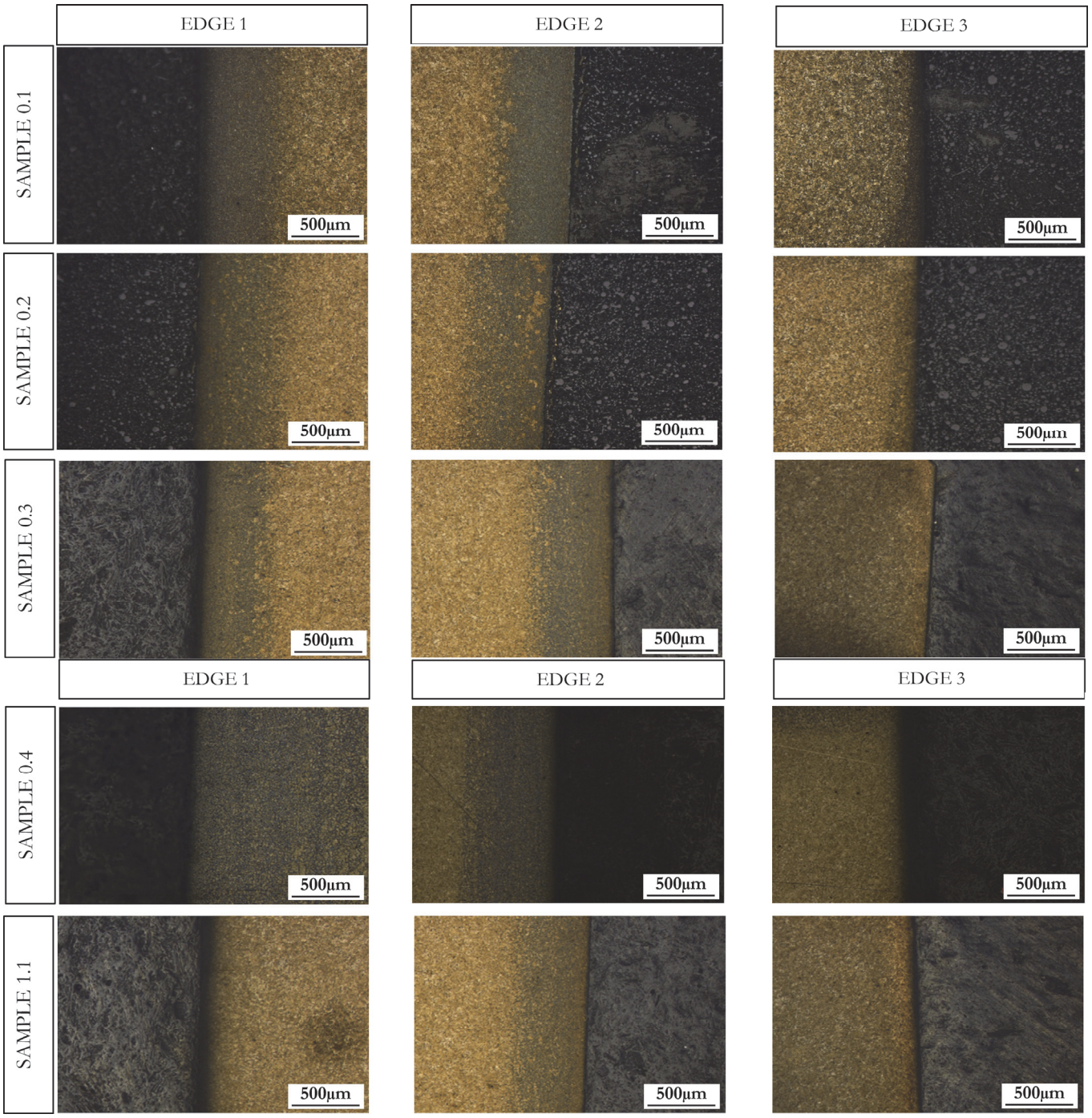

Figure 5: Micrographs of samples from Set #1 (etching agent: Nital2 - optical microscope). The images show the microstructure under the surface of edge 1, 2 and 3 of samples 0.1, 0.2, 0.3, 0.4 and 1.1 at low magnification (25x).

The samples in Set #1 were also analysed chemically. Tests were performed at increasing distances from the surface to know the amount of carbon and boron along the sample thickness. The results are summarized in Fig. 6.
The carbon content is almost constant all along the thickness and there is no evidence of decarburization [11]. Compared to carbon, boron exhibits a fluctuating trend. Actually, it is quite stable (0.0025%-0.0029%) down to a depth of 0.3mm from the surface, then increases to about 0.0038% at a depth of 0.35mm and then sharply decreases (about 0.0015%) at 0.7mm from the surface. Below 0.7mm, boron stabilizes around the standard value (0.0025%) measured in the base material. Almost all boron is in solution in the metal lattice; only a negligible part of it is not in solution at a depth between 0.3mm and 0.7mm. In any case, the chemical analysis revealed a boron content higher than 0.0015% [4] that is the minimum amount required to activate the hardenability improvement in carbon steel.

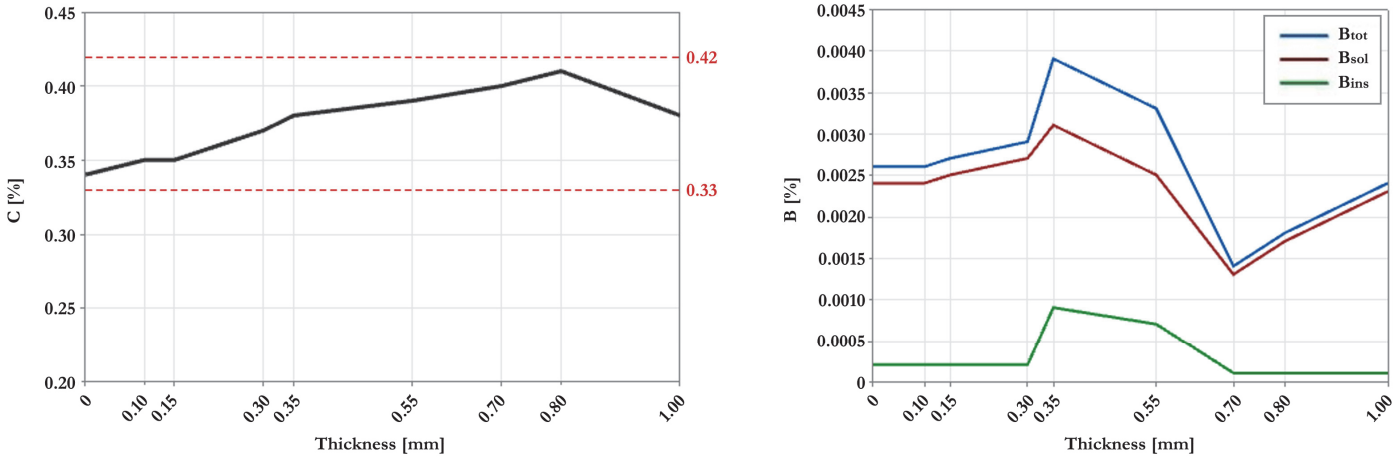

Figure 6: Chemical analysis of sample 0.1; the images show the trend of carbon (left) and boron (right) along the sample thickness.

Set #2

Fig. 7 shows the microstructure of A.X samples. Equiaxed grains of pearlite and ferrite characterize sample A.1 (As-Rolled + Pickling); the metallographies also show a small amount of titanium nitrides of micrometric dimension (1-5µm) along the entire thickness (red boxes in Fig. 7). These compounds still exist after the spheroidize annealing treatments (samples A.2 and A.3). Titanium nitrides observed in A.X samples are quite common in boron steel [12] where the titanium addition is performed to inhibit the formation of boron nitrides that would impair steel hardenability.

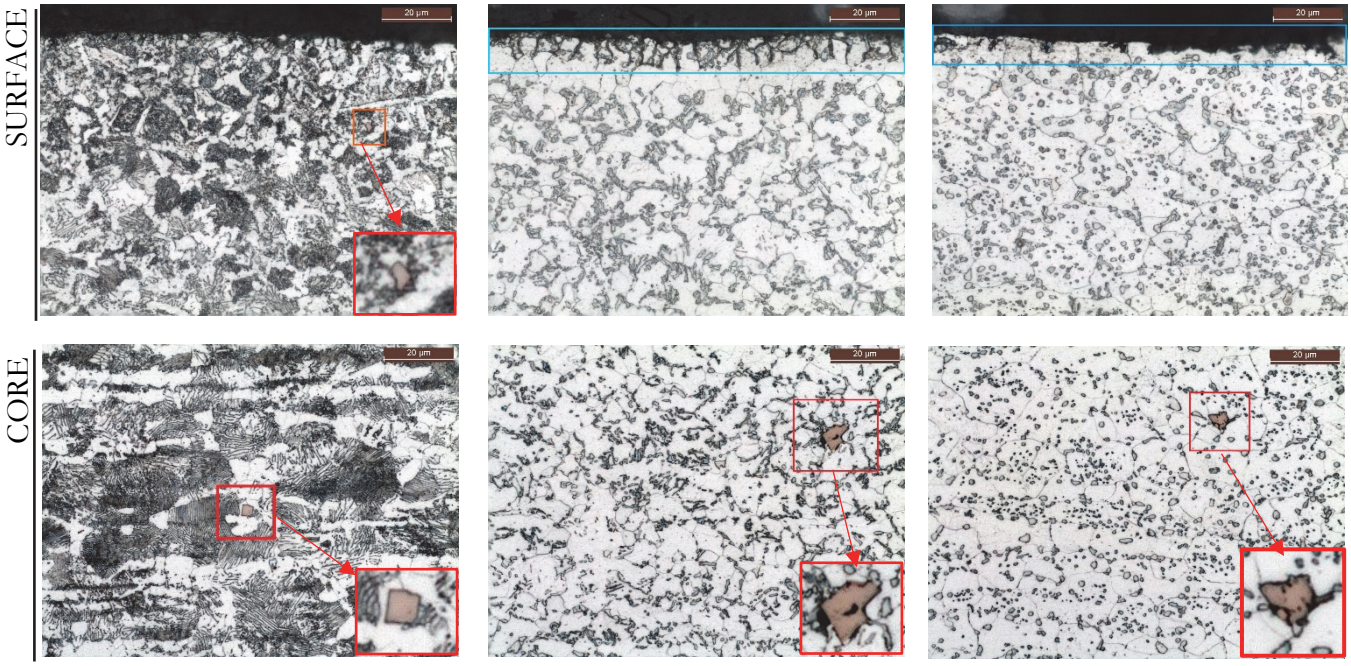

a) Sample A.1 b) Sample A.2 c) Sample A.3

Figure 7: Micrographs of A.X samples (etching agent: Nital2 - optical microscope). The images show the microstructure below the surface and at the core of samples A.1, A.2 and A.3 at 1,000x magnification.

Samples A.2 and A.3 exhibit a thin oxidized layer (< 20 µm) below the surface (light blue lines in Fig. 7), showing slight oxygen contamination of the H_2-N_2 protective atmosphere used for spheroidize annealing.

The SEM analyses of A.X samples (Figs. 8 and 9) reveal other types of compounds finely scattered both inside and at the boundaries of the ferritic grains. These compounds mainly consist of nitrides, carbides, or carbo-nitrides of titanium, aluminum or silicon with nanometric dimension (<< 1µm). The compounds are mainly localized below the surface (orange dashed lines and red boxes in Fig. 9) while they are almost absent at the core of the sample. Metallographies show that nanometric compounds increase sharply after spheroidize annealing heat treatments.

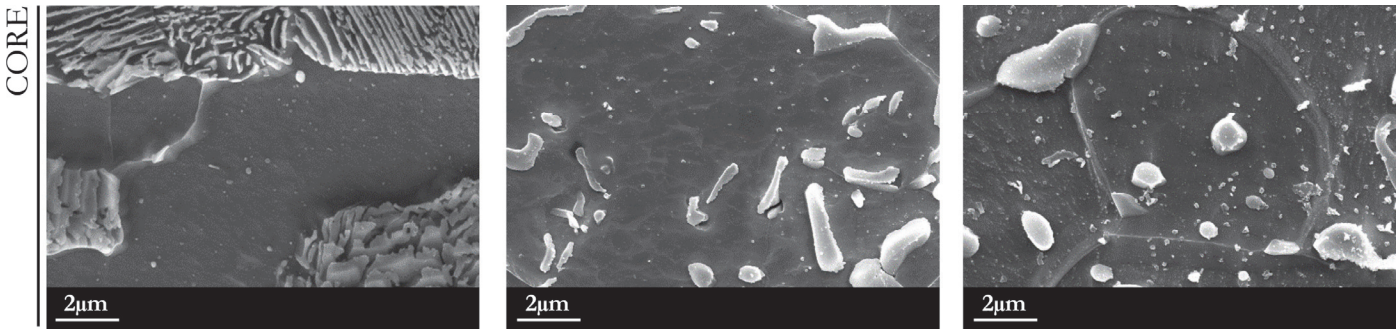

a) Sample A.1 b) Sample A.2 c) Sample A.3

Figure 8: Micrographs of A.X samples. SEM analyses at the core (magnification: 20,000x - etching agent: Nital2).

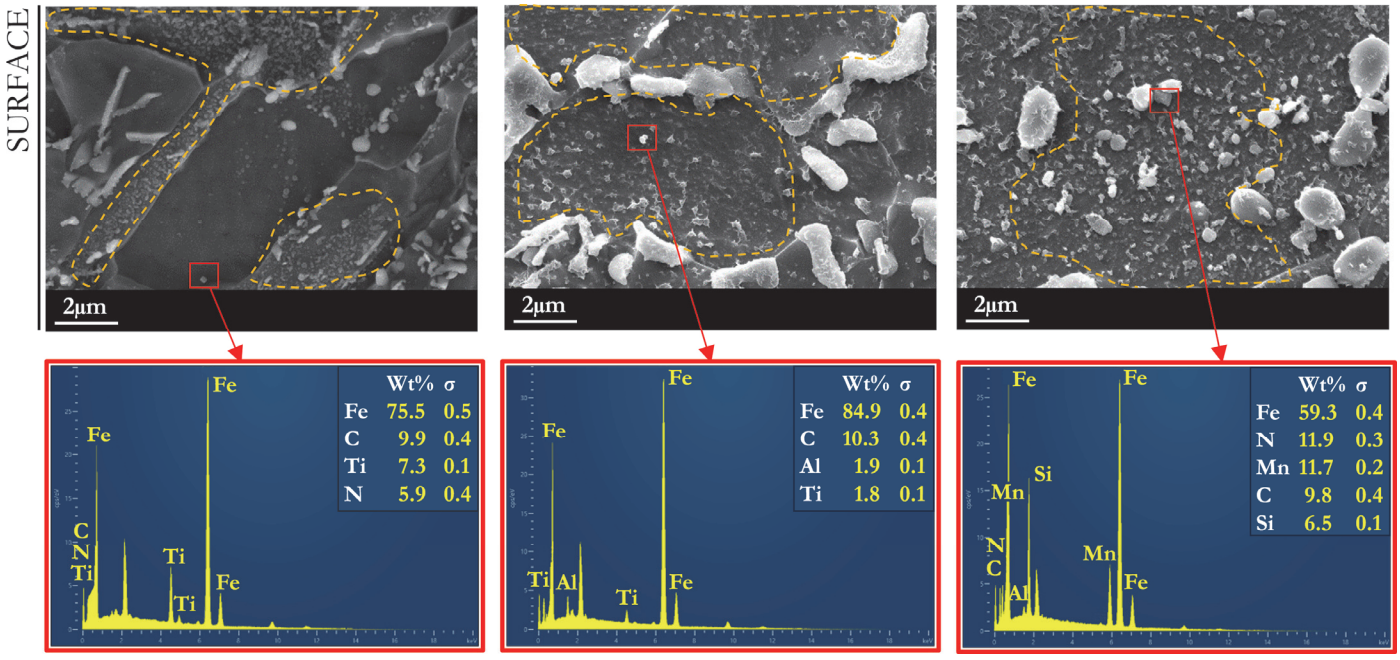

a) Sample A.1 b) Sample A.2 c) Sample A.3

Figure 9: Micrographs of A.X samples. SEM analyses at 0.2mm depth from the surface (magnification: 20,000x - etching agent: Nital2). The orange dashed lines highlight areas characterized by nanometric compounds. The red boxes indicate the compound chemical analysis.

Nanometric compounds do not dissolve at quenching or spheroidize annealing temperatures (880°C and 700°C, respectively) and act as nucleation sites for new grains when heat treatments exceed steel critical points. The great number of nucleation sites causes strong grain refinement and decreases hardenability beneath the surface.

The chemical analysis performed on sample surfaces shows an increase in the nitrogen content from sample A.1 (0.0064%) to sample A.2 (0.0190%) and sample A.3 (0.0460%). The nitrogen content on the surface of samples A.2 and A.3 exceeds the level between 0.0040% and 0.0070%, which is considered acceptable in steels [13], by an order of magnitude.

Conversely, the level of boron in solution in the metal lattice shows an opposite trend as it decreases from samples A.1 to samples A.2 and A.3. In any case, the level of boron in solution is above the minimum amount of 0.0015%.

Chemical analyses in Tab. 3 highlight that the progressive increase of nanometric compounds follows the increase of nitrogen beneath the surface. This indicates a contamination of undissociated NH_3 in the H_2-N_2 protective atmosphere used for spheroidize annealing. When, following contamination, small traces of ammonia come in contact with steel at high temperature, they break down into atomic nitrogen (N) and molecular hydrogen (H_2), which creates the condition for the formation of a small amount of nitrides beneath the surface.

Finally, Fig. 10 shows the samples after the Q&T treatments. As expected, the layer of very fine ferrite and pearlite already found in the samples from Set #1 is also present in samples A.1.1, A.2.1 and A.3.1 (red dashed lines in Fig. 10). This layer

is negligible (0.1mm depth) in sample A.1.1 where it causes a limited hardness decrease equal to 50HV (Fig. 10.a). Sample A.2.1 shows a deeper layer of ferrite and pearlite (down to 0.3mm) and a more considerable loss of hardness, about 100HV, not compliant with the minimum hardness requirement (Fig. 10.b). Sample A.3.1 shows a loss of hardness and thickness of the ferrite and pearlite layer that are even worse than in sample A.2.1. The decrease in hardness is about 150HV and the layer depth is about 0.6mm.
The SEM analysis of sample A.3.1 confirms that martensite transformation does not occur beneath the surface where the nanometric compounds inside the ferrite grain are still present after Q&T while the core of sample A.3.1 is composed exclusively of martensite.

	C [%]	Si [%]	Mn [%]	P [%]	S [%]	Cr [%]	Mo [%]	Ni [%]	Al [%]	Cu [%]	Ti [%]	B_{sol} [%]	B_{tot} [%]	N [%]
Sample A.1	0.35	0.24	1.30	0.014	0.002	0.13	0.02	0.02	0.033	0.040	0.036	0.0024	0.0025	0.0064
Sample A.2	0.34	0.23	1.29	0.013	0.002	0.12	0.02	0.02	0.028	0.041	0.034	0.0020	0.0023	0.0190
Sample A.3	0.35	0.24	1.28	0.013	0.002	0.12	0.02	0.02	0.022	0.040	0.034	0.0018	0.0024	0.0460

Table 3: Chemical analysis at the surface of A.X samples (EN 34MnB5 steel).

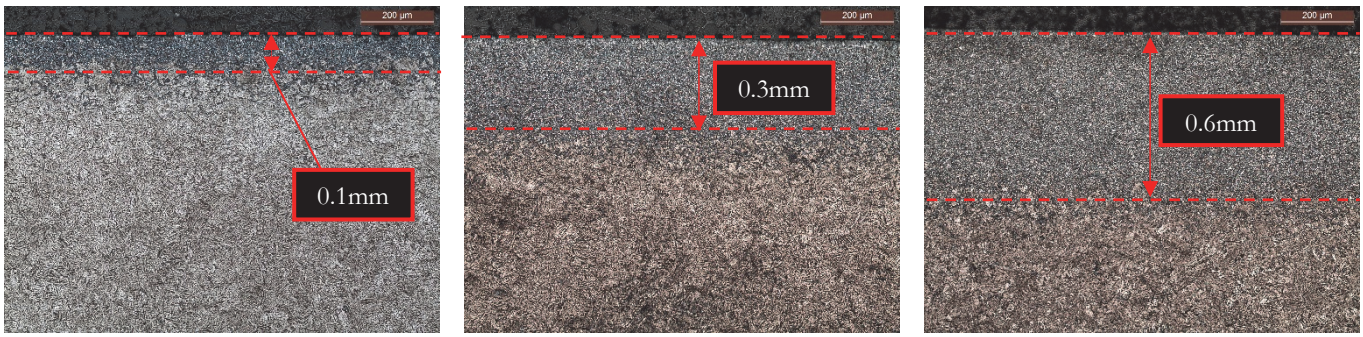

a) Sample A.1.1 b) Sample A.2.1 c) Sample A.3.1

Figure 10: Micrographs of A.X.1 samples after Q&T (etching agent: Nital2 - optical microscope). The images show the microstructure below the surface of samples A.1.1, A.2.1 and A.3.1 at 200x magnification.

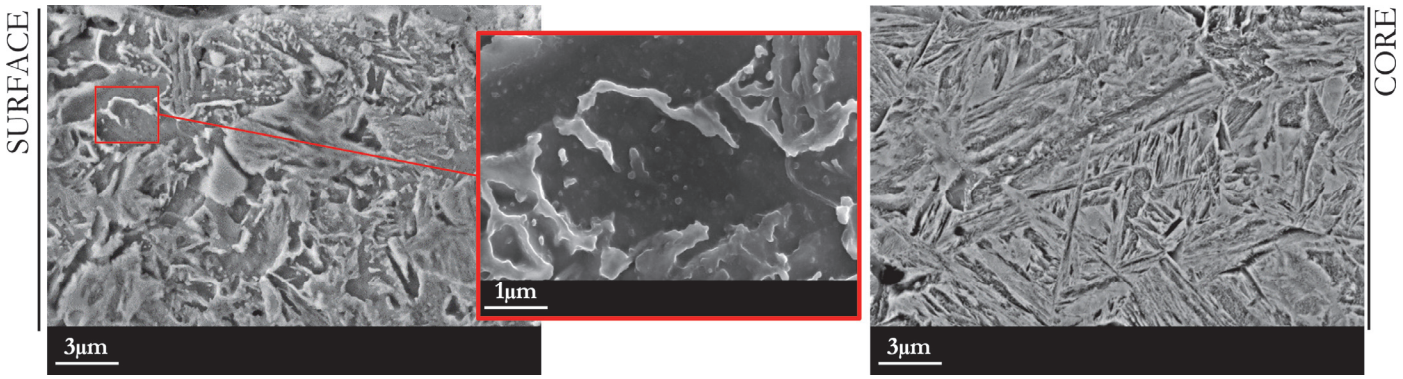

Figure 11: Micrographs of A.3.1 samples (magnification: 10.000x – etching agent: Nital2). SEM analyses below the surface (left) and at the core (right).

Set #3

Tab. 4 shows the chemical analysis performed on the 10 samples in Set #3. The first five samples were used to produce non-compliant components (batch B.1) while the remaining five were used to produce components meeting the minimum surface hardness requirement after Q&T (batch B.2).

The chemical analysis shows that all five samples from batch B.1 have an extremely high level of nitrogen at a depth of 0.2mm from the surface. Then, the nitrogen content sharply decreases as you move away from the surface, reaching a level slightly above the acceptable limit at 1.0mm depth from the surface. On the other hand, batch B.2 has a low nitrogen content, ranging from 0.0040%-0.0070%, both below and far from the surface.
The samples in Set #3 confirm that non-compliant components always come with a nitrogen level under the surface that exceeds the correct amount by an order of magnitude.

Batch	Surface Hardness [HV]	Compliant	C	Si	Mn	Cr	Ni	Ti	%N [depth: 0.2 mm]	%N [depth: 1.0 mm]
B.1	301-319	No	0.22	0.34	1.13	0.30	0.02	0.033	0.0361	0.0078
B.1	283-312	No	0.22	0.34	1.12	0.30	0.02	0.031	0.0383	0.0072
B.1	286-317	No	0.23	0.34	1.13	0.30	0.02	0.033	0.0354	0.0069
B.1	291-326	No	0.22	0.35	1.14	0.30	0.02	0.033	0.0412	0.0080
B.1	293-322	No	0.22	0.35	1.15	0.31	0.02	0.033	0.0378	0.0071
B.2	414-446	Yes	0.27	0.22	1.30	0.20	0.05	0.056	0.0063	0.0055
B.2	430-437	Yes	0.25	0.22	1.30	0.20	0.05	0.056	0.0058	0.0050
B.2	417-442	Yes	0.26	0.22	1.31	0.20	0.05	0.056	0.0065	0.0054
B.2	422-427	Yes	0.26	0.22	1.31	0.20	0.05	0.057	0.0060	0.0052
B.2	419-431	Yes	0.26	0.22	1.31	0.20	0.05	0.056	0.0069	0.0057

Table 4: Chemical analysis of samples from Set #3.

Conclusions

The combination of fine blanking and boron steel was analysed to show some drawbacks that can occur during heat treatments of automotive components. An experimental campaign was performed on two different boron steels, namely EN 34MnB5 and EN 22MnB5. The steel samples were previously spheroidized annealed in a neutral environment (hydrogen/nitrogen atmosphere), then fine blanked to obtain specific automotive components which were subsequently quenched and tempered.
Experimental tests revealed precipitation of nanometric compounds which act as nucleation sites for new grains when subjected to heat treatments above critical points. This effect blocks grain growth, triggers strong refinement of the grains and drastically decreases the hardenability of components. Moreover, the nanometric boron compounds diminish free boron, further reducing hardenability under the surface.
The compounds are mainly localized below the surface and are almost absent at the core of the sample. Hardenability problems were brought back to nitrogen pick-up during initial spheroidize annealing treatments. The chemical analysis highlights that the progressive increase of nanometric compounds matches nitrogen increase beneath the surface, indicating a contamination of undissociated NH_3 in the H_2-N_2 protective atmosphere used for spheroidize annealing. When, following contamination, small traces of ammonia come in contact with steel at high temperature, they break down into atomic nitrogen (N) and molecular hydrogen (H_2), which creates the condition for the formation of a small amount of nitrides beneath the surface.
All non-compliant samples have a nitrogen level beneath the surface (down to a depth of 0.7mm) that exceeds the correct amount (0.0040%-0.0070%) by an order of magnitude. The nitrogen content sharply decreases as you move away from the surface, reaching a level slightly above the acceptable limit at a depth of 1.0mm from the surface.

REFERENCES

[1] Ali, M., Nyo, T.T., Kaijalainen, A., Javaheri, V. (2021). Incompatible effects of B and B + Nb additions and inclusions' characteristics on the microstructures and mechanical properties of low-carbon steels. Materials Science and Engineering A, 819, 141453.

[2] Harries, D.R., Marwick, A.D. (1980). Non-equilibrium segregation in metals and alloys. Philosophical Transactions of the Royal Society of London. Series A, Mathematical and Physical Sciences, 295(1413), pp. 197-207.

[3] Bercovici, S.J., Hunt, C. E. L., Niessen, P. (1970). A Model of Vacancy Flux Induced Segregation to Grain-Boundaries During Cooling. Journal of Materials Science, 5, pp. 326-330.

[4] Sharma, M., Ortlepp, I., Bleck, W. (2019). Boron in Heat-treatable Steels: A Review. Steel Research International, 90(11), 1900133.

[5] Opiela M. (2019). Effect of boron microaddition on hardenability of new-developed HSLA-type steels. Archives of Materials Science and Engineering, 99(1/2), pp. 13-23.

[6] Zheng, Q., Zhuang, X., Zhao, Z. (2019). State-of-the-art and future challenge in fine-blanking technology. Production Engineering, 13, pp. 61-70.

[7] Nielsen, C.V., Alves, L.M., Bay, N., Martins P.A.F. (2021). Tool Design, In: Metal forming: Formability, Simulation, and Tool Design, London, Elsevier, pp. 277-370.

[8] Jia, T., Li, M., Pei, X., Wang Z. (2019). On the Spheroidizing Annealing Behavior in Cr/Nb Microalloyed Medium Carbon Steels. Steel Research International, 90(2), 1800353.

[9] Moisă, B.A., Chiran, A., Priceputu, I., Bacinschi Z. (2011). The controlled atmosphere influence over the aspect of the stainless steel strip. Materials and Mechanics, 6, pp. 63-69.

[10] Aravind, U., Chakkingal, U., Venugopal, P. (2021). A review of fine blanking: Influence of die design and process parameters on edge quality. Journal of Materials Engineering and Performance, 30, pp. 1-32.

[11] Katok, O.A., Muzyka, M.R., Shvets', V.P., Sereda, A.V., Kharchenko, V.V., Bisyk, S.P. (2021). Determination of Hardness of High-Strength Steels by the Brinell Method. Part 1. Improvement of Measurement Accuracy. Strength of Materials, 53(6), pp. 902-908.

[12] Capurro, C., Cicutti, C.E. (2018). Analysis of titanium nitrides precipitated during medium carbon steels solidification. Journal of Materials Research and Technology, 7(3), pp. 342-349.

[13] Zhao, Y., Yang, Y., Barati, M., McLean A. (2018). Strategies for nitrogen control during the production of interstitial-free steel. Ironmaking and Steelmaking, 45(6), pp. 485-491.